CellPress
OPEN ACCESS

Trends in
Cancer

Review

Serrated colorectal cancer: preclinical models and molecular pathways

Aziz Aiderus [1,*] Nick Barker,[2,3] and Vinay Tergaonkar[1,4]

Serrated lesions are histologically heterogeneous, and detection can be challenging as these lesions have subtle features that may be missed by endoscopy. Furthermore, while approximately 30% of colorectal cancers (CRCs) arise from serrated lesions, only 8–10% of invasive serrated CRCs exhibit serrated morphology at presentation, suggesting potential loss of apparent characteristics with increased malignancy. Thus, understanding the genetic basis driving serrated CRC initiation and progression is critical to improve diagnosis and identify therapeutic biomarkers and targets to guide disease management. This review discusses the preclinical models of serrated CRCs reported to date and how these systems have been used to provide mechanistic insights into tumor initiation, progression, and novel treatment targets.

Highlights

The 'serrated' pathway is an alternative route to the development of colorectal cancers (CRCs) with unique features such as enrichment of *BRAF* mutations, extensive CpG island methylation, and microsatellite instability.

Activating mutations in *BRAF* are enriched in serrated CRC and proposed as the initiating genetic event. However, BRAF activation alone is insufficient for tumorigenesis, and the additional events required for disease progression are poorly understood.

In vivo and *in vitro* models have been useful in the reenactment of the stepwise genetic events and mechanistic studies underpinning tumorigenesis.

However, the tumor location and molecular features of serrated CRC requires careful selection of Cre lines for targeting *in vivo* genetic events to ensure that tumors which arise faithfully recapitulate features of human disease.

Organoid models also require incorporation of external factors such as the stromal and immune cells, as well as components of the microbiome, to closely mimic human disease.

Clinical and molecular features of serrated CRC

The earliest description of serrated adenomas appeared in the 1990s [1], but these entities were largely ignored in clinical practice due to a poor understanding of the histology and underlying molecular features. Since 2000, several studies further defined the morphology and molecular correlates of these lesions and demonstrated a link between sessile serrated adenoma and cancer risk [2–6].

Up to 30% of sporadic CRCs develop through the serrated pathway [7], and they are among the primary causes of interval cancers (defined as CRC diagnosed within 60 months of a negative colonoscopy) [8–11] and are associated with synchronous (second cancer diagnosed within 6 months of primary cancer diagnosis) and metachronous (second cancer diagnosed >6 months after first cancer diagnosis) cancers. Epidemiologically, **serrated CRCs** (see Glossary) occur more frequently in the elderly, often women, and on the right side of the colon. The fifth edition of the World Health Organization Classification of Tumors of the Digestive System [12] classified serrated colorectal lesions into three categories: (i) hyperplastic polyps (HPPs), sessile serrated lesions (SSLs) with or without dysplasia, and (iii) traditional serrated adenoma/polyp (TSA).

HPPs are the most common form of serrated polyps, accounting for between 60% and 75% of serrated lesions. HPPs are typically small (<5 mm), located on the left side of the colon, and present with a flat or sessile morphology. The crypts of HPP are straight and elongated, with the upper two-thirds exhibiting serrated architecture and minimal cytological atypia. The bottom third of the crypt is regular with neither serrations nor atypia. HPPs can be further subclassified on the basis of mucin type into microvesicular hyperplastic polyps (MVHPs) and goblet cell-rich hyperplastic polyps (GCHPs). MVHPs make up approximately 60% of HPPs and share molecular features with SSLs. By contrast, GCHPs comprise ~30% of HPPs and are more related to TSAs at the molecular level. SSLs account for between 20% and 35% of all serrated lesions, are devoid of adenomatous alterations, and are generally flat compared with the more commonly observed

[1]Laboratory of NFκB Signalling, Institute of Molecular and Cell Biology (IMCB), Agency for Science, Technology and Research (A*STAR), 61 Biopolis Drive, Proteos, Singapore 138673, Republic of Singapore
[2]Department of Physiology, Yong Loo Lin School of Medicine, National University of Singapore (NUS), 2 Medical Drive, MD9, Singapore 117593, Republic of Singapore
[3]Institute of Molecular and Cell Biology (IMCB), Agency for Science, Technology and Research (A*STAR), 61 Biopolis Drive, Proteos, Singapore 138673, Republic of Singapore

pedunculated polypoid conventional adenoma. SSLs are frequently located on the right side (proximal), although between 20% and 40% have been reported to present distally (left side). SSLs range between 5 and 10 mm in diameter and can be subclassified into lesions with and without dysplasia. Approximately 4–8% of SSLs have a dysplastic focus, characterized by eosinophilic cytoplasm and small glands that are tightly packed. There are several histopathologic features important for identifying SSLs: (i) a T- or L-shaped horizontal growth along the muscularis mucosa, (ii) dilated bottom third of the crypt base with serrations extending into it, and (iii) shift in the proliferation zone from the crypt base to the dilated, lateral side. TSAs are the least common and account for <1% of all serrated lesions, typically >5 mm in diameter and localized to the distal colon. In contrast to HP and SSA/P, TSAs can present with either a sessile or pedunculated shape. These lesions present histologically with a distorted villous or tubulovillous architecture, with the villi frequently having bulbous tips.

In contrast to CRC that develops via the conventional pathway, serrated CRCs rarely present with mutations in the *APC* and *KRAS* genes and are chromosomally stable (Figure 1). However, despite the lack of inactivating *APC* mutations, Wnt signaling can be activated via other mechanisms, such as via inactivating mutations in *RNF43* [13,14]. Serrated CRCs are enriched in the $BRAF^{V600E}$ activating mutation and are strongly associated with **microsatellite instability (MSI)** and the **CpG island methylator phenotype (CIMP)**. MSI occurs due to a **deficient mismatch repair (dMMR)** pathway via epigenetic silencing or inactivating mutations in genes in the pathway. The most common event is the methylation of promoter sites upstream of *MLH1* as well as inactivating germline mutations in other MMR genes, such as *MSH2*, *MLH1*, *MSH6*, *PMS2*, and *PMS1*, particularly in hereditary nonpolyposis CRC [15]. Of note, a smaller proportion of serrated CRC are microsatellite stable (MSS) and correlates with poor prognosis [16]. CIMP status is determined on the basis of assessment of the methylation

[4]Department of Biochemistry, Yong Loo Lin School of Medicine, National University of Singapore (NUS), 8 Medical Drive, MD7, Singapore 117596, Republic of Singapore

*Correspondence:
abdul_aziz_aiderus@imcb.a-star.edu.sg
(A. Aiderus).

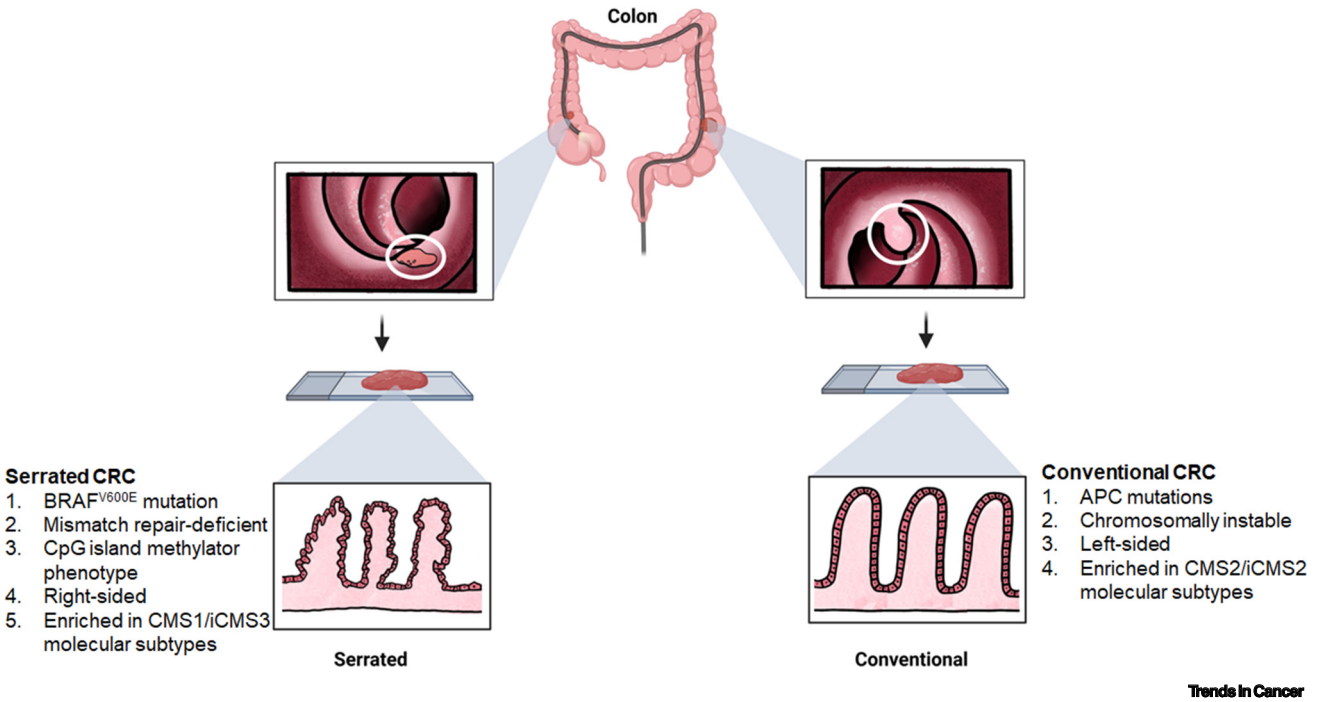

Figure 1. Key features between serrated and conventional colorectal cancer (CRC). The salient clinical and molecular features associated with each lesion type are indicated.

levels of five genes and methylation of at least three genes is considered CIMP-high, whereas methylation of one or two genes is considered CIMP-low [17,18]. Other panels have also been proposed [19], which presents a challenge when comparing CIMP status across different studies. Altogether, serrated CRCs exhibit enrichment in features that occur in a relatively small proportion of all CRC cases, with implications for early detection and adjuvant treatment. Molecular subtypes have been reported for CRCs, and serrated CRCs are enriched in the consensus molecular subtype 1 and the more recently defined intrinsic molecular subtype 3 [20,21].

While the clinical correlates of serrated CRC are well defined, an in-depth understanding of the genetics and signaling pathways driving tumor development is lacking. Preclinical models have proved essential in understanding tumorigenesis and response to various treatment modalities [22], and recent studies have detailed the initiation and progression mechanisms involved in serrated CRC development. This review aims to synthesize the various preclinical models reported to date, with a focus on genetically engineered mouse models. In doing so, we highlight the biological processes and pathways essential for serrated CRC development in *in vitro* and *in vivo* models and propose avenues for future investigation.

Preclinical models of serrated CRC

Braf^{V600E} is a key initiating hit in driving precursor serrated lesions

Activating mutations in the *BRAF* proto-oncogene occur in over 60% of precursor hyperplastic or serrated crypt foci compared with only 6% in nonserrated lesions, suggestive of an initiating role for the BRAF^{V600E} mutation in early serrated lesions [23]. The most common mutation is CTG→CAG at nucleotide 1799, which results in an amino acid substitution from valine to glutamic acid at residue 600 located in exon 15. This generates a constitutively active enzyme estimated to have 500-fold kinase activity relative to the wild-type molecule [24].

One of the earliest studies to functionally demonstrate the initiating role of Braf^{V637E} (the human ortholog of BRAF^{V600E}) used AhCre^{ERT2} mice to activate oncogenic Braf in the intestinal stem and transit amplifying cells [25]. The conditional activation of the kinase resulted in an initial burst of hyperproliferation, resulting in HPP lesions that subsequently entered senescence driven by the p16 tumor suppressor. Indeed, deletion of *Cdkn2a* (that encodes the p16 protein) bypassed this dormancy to drive progression to invasive serrated CRC. A second study used *Villin*-Cre mice to drive intestinal tissue-specific expression of Braf$^{Lox\text{-}Stop\text{-}Lox(LSL)\text{-}V637E/+}$ [26]. This resulted in persistent, lifelong crypt hyperplasia, which was characterized by serrated epithelial features, with morphological similarities to human MVHP or GCHP. Furthermore, hyperplasia-to-dysplasia progression was observed as early as 2 months, at which point some animals had already developed macroscopic masses. However, only one of 12 (8%) of the *Vil*-Cre*;Braf*$^{LSL\text{-}V637E/+}$ mice younger than 10 months and four of 29 (13.8%) older than 10 months developed invasive cancers, of which two were low-grade (well/moderately differentiated) and three were high-grade (poorly or undifferentiated, with <50% of tumors exhibiting glandular structures). These findings were independently corroborated in a separate study that employed transgenic expression of a doxycycline-inducible version of the Braf^{V600K}. Consistent with the previous two studies, this led to dramatic changes in the intestinal morphology (e.g., saw-toothed villi, tufts of aggregated enterocytes of villus tip, loss of basal positioning of nuclei in the epithelium, enlarged nuclei, and increased nuclei-to-cytoplasm ratio) [27]. It is worth mentioning that *KRAS* mutations have been detected in serrated lesions [28] and *Vil*-Cre-driven activation of oncogenic Kras in mouse intestine resulted in serrated hyperplasia and senescence [29]. Collectively, these findings suggest that Braf activation [or activation of the mitogen-activated protein kinase (MAPK) pathway] is sufficient to initiate intestinal hyperplasia, which inefficiently progresses to invasive cancers in the absence of additional genetic events [30].

Glossary

CpG island methylator phenotype (CIMP): extensive methylation of CpG island of promoter sites. Typically, this serves to silence the expression of tumor suppressor genes, thereby supporting tumor development.
Deficient mismatch repair deficiency (dMMR): inactivation of the MMR pathway due to methylation at promoter site of genes such as *MLH1*.
Microsatellite instability (MSI): short tracts of DNA that are repeated and prone to replication error, which can be repaired if the MMR system is functional. However, when the MMR pathway is inactive (via methylation of genes encoding repair enzymes), it results in altered length of microsatellite sequences, giving rise to MSI.
Serrated CRC: an alternative route to CRC development, compared with the more common 'conventional' route (which is driven by *APC* mutations). Serrated CRCs have a distinct histology, marked by a 'saw-toothed' crypt structure that starts from the top of the crypt and may progress all the way to the base.

While mouse models are useful to study serrated CRC development, the time taken for tumorigenesis presents a challenge to performing genetic screens and short-term therapeutic studies. Recently, organoid systems have been proposed as an alternative to model disease development [31]. Organoid cultures of patient-derived HP and SSA/P were originally reported by Toshiro Sato's group [32]. Subsequently, colon organoids from *Villin*-Cre;Braf^{V637E} mice were established and treated with 4-hydroxytamoxifen to induce oncogenic kinase activity [33], thereby establishing an *in vitro* system to study serrated CRC development. The authors then tested stepwise disruption of *Tgfbr2*, *Rnf43*, *Znrf3*, *p16Ink4a*, and *Mlh1* via the CRISPR-Cas9 system. Orthotopic transplant of organoids with only Braf activation did not generate tumors, whereas Braf activation combined with inactivating mutations in *Tgfbr2*, *Cdkn2a*, *Znrf2*, and *Rnf43* resulted in frequent tumor formation (57–100%), with greater tumor formation rates associated with increasing numbers of genetic alterations. A separate study modelled the rarer human TSA by performing chromosome engineering to model *RSPO1* gene fusions using human colonic organoids, as well as genetic alterations in *TP53*, *BRAF*, and *GREM1* [34]. Organoids harboring BRAF^{V600E} and R-spondin 1 fusions formed flat serrated lesions in mice, whereas organoids with BRAF^{V600E}, R-spondin 1 fusions, and GREM1 overexpression formed tumors that exhibited features of human TSA. Collectively, these studies demonstrate that the organoid system recapitulates some features of human serrated CRC and may be useful models for genetic and pharmacologic screens.

A general limitation of tumor organoids has been the absence of other cell types, including stroma, vasculature, and immune cells [31]. These cell types are likely to be complicit in tumorigenesis and therefore may affect interpretation of mechanistic studies as well as pharmacologic screens, which necessitates more complex organoid systems. More recent examples include the successful culture of tumor organoids with fibroblasts or immune cells in pancreatic ductal adenocarcinoma, renal cell and non-small cell lung carcinomas, and melanoma, as well as the coculture of fibroblasts with mouse tumor organoids or CRC cells to form 3D organotypic growth [35–39]. The cell types to include in organoid generation and culture can be prioritized from single-cell and/or spatial transcriptomic analyses of serrated polyps and tumors from patients. Ligand–receptor interaction analysis may identify key mediators of interactions between the tumor epithelium and its environment; key cell types can be isolated and cocultured with the tumor organoids.

Braf^{V600E} activation, aging, and global genomic hypermethylation

Approximately half of SSLs exhibit CIMP, and the majority of advanced dysplastic SSLs are also CIMP-positive, indicating that CIMP is necessary and occurs early during SSL evolution. Analyses of patient material in three studies demonstrated a strong association between *BRAF* mutation and CIMP-high serrated polyp and CRC compared with CIMP-low polyps and CRC, suggesting an association between BRAF activation and global genomic hypermethylation [5,19,40].

Early studies have shown a strong association between BRAF^{V600E} and accumulation of epigenetic marks that facilitate transformation and serrated CRC development [5,41]. How does BRAF^{V600E} activation drive global hypermethylation? Although the mechanistic understanding is incomplete, one possible explanation was provided by a study that performed an RNAi screen to identify mediators of *MLH1* silencing and identified *MAFG* (MAF BZIP transcription factor G) as a strong candidate [42]. Since the RKO cell line used for this screen harbors the BRAF^{V600E} mutation, the authors assessed whether inhibition of the kinase activity affects MAFG, its interaction with other corepressors, and *MLH1* silencing. Pharmacologic or genetic inhibition of BRAF^{V600E} resulted in decreased MAFG expression and decreased *MLH1* methylation in the RKO cell line.

Additionally, overexpression of $BRAF^{V600E}$ in primary foreskin fibroblasts increased MAFG levels and reduced MLH1 expression. Mechanistic experiments demonstrated that extracellular signal-regulated kinase (ERK)-dependent phosphorylation promotes MAFG stability against proteasomal degradation, and ChIP analysis revealed that MAFG interacts with BACH1 to recruit corepressors such as DNMT3B and CHD8 to the complex.

Since then, several studies have provided experimental evidence for a direct role of $Braf^{V600E}$ activation and gene promoter hypermethylation using higher model systems, such as genetically engineered mouse and organoid cultures. For example, intestine-specific activation of $Braf^{V600E}$ in mice resulted in a time-dependent increase in promoter hypermethylation of a predefined gene panel [43]. Taking this study further, organoids were derived from the proximal colon of $Braf^{V600E}$ mice and initial passages of the organoids underwent cell death [44]. However, longer-term (11 weeks) culture of the organoids in medium with niche factors, including epidermal growth factor (EGF), Noggin, R-Spondin 1, and Wnt3a, resulted in growth with neoplastic phenotypic changes such as dysplasia and cryptlike stem cell buds growing inwards, with polypoid growth filling the inner lumen. Long-term culture (5 months) generated organoids that acquired independence from the niche factors with profound global methylation changes in negative regulators of Wnt signaling, $p16^{Ink4a}$, a key suppressor of senescence, and *Cdx2*, a CRC tumor suppressor gene. Many of the methylated genes observed in the $Braf^{V600E}$ organoids were strongly conserved in human proximal CRC that were CIMP-positive, suggesting the clinical relevance of this model system. Of note, longer-term culture (12–14 months) of empty vector (wild-type control) organoids resulted in independence from Noggin or Wnt3a supplementation and exhibited promoter methylation in the same set of genes in $Braf^{V600E}$ organoids cultured for 5 months.

Considering these findings, the relationship between aging, DNA methylation, and BRAF activation [45] was assessed by profiling the DNA methylation status of murine proximal small intestine between 24 days and 20 months after weaning. Eight percent of global CpG sites were significantly associated with aging, termed as type A (age-associated), including in 105 tumor suppressor genes such as *Cdkn2a* and *Dkk3*. There was limited overlap between the methylation profile of this study and the study described earlier [43], which may be due to prolonged culture environment in the latter, gender differences in animals, and different tissue origin between studies (small intestine here vs. colon [43]). Further analysis of age-associated DNA methylation in mice with $Braf^{V600E}$ activation from 10 days to 14 months after weaning revealed that 16.8% of global CpG sites were associated with aging, of which 81.3% were components of the type A sites. Furthermore, Braf activation resulted in differential rates of methylation in 69.5% of age-associated CpG sites, termed type AB (age associated and modified by Braf activation). Type AB gene promoters also demonstrated a stronger enrichment for WNT signaling compared with type A, suggesting an interaction between aging and Braf/MAPK activation in selecting for epigenetic regulation of WNT signaling in the mouse small intestine. This finding also challenged the prevailing view that serrated CRC develops over time after BRAF activation and initiation of serrated lesions. Indeed, the incidence of serrated lesions was approximately tenfold higher (43.8% vs. 4.2%) in animals that were aged 9 months before activating Braf for 5 months ($Braf^{9-14}$) compared with mice with Braf activation for 5 months after weaning ($Braf^{W-5}$), suggesting that aged intestine markedly alters the proclivity to Braf-induced serrated neoplasia. Altogether, these findings suggest that aging and its associated intestinal epigenetic alterations can rapidly drive serrated lesions following BRAF activation.

Genetic hits and pathways associated with serrated CRC progression

$BRAF^{V600E}$ plays a key role in the initiation of serrated polyps. However, the genetic events that drive progression of benign lesions to malignant serrated CRC are poorly understood. In this

Key figure

Pathways implicated in serrated colorectal cancer (CRC) development from *in vivo* studies

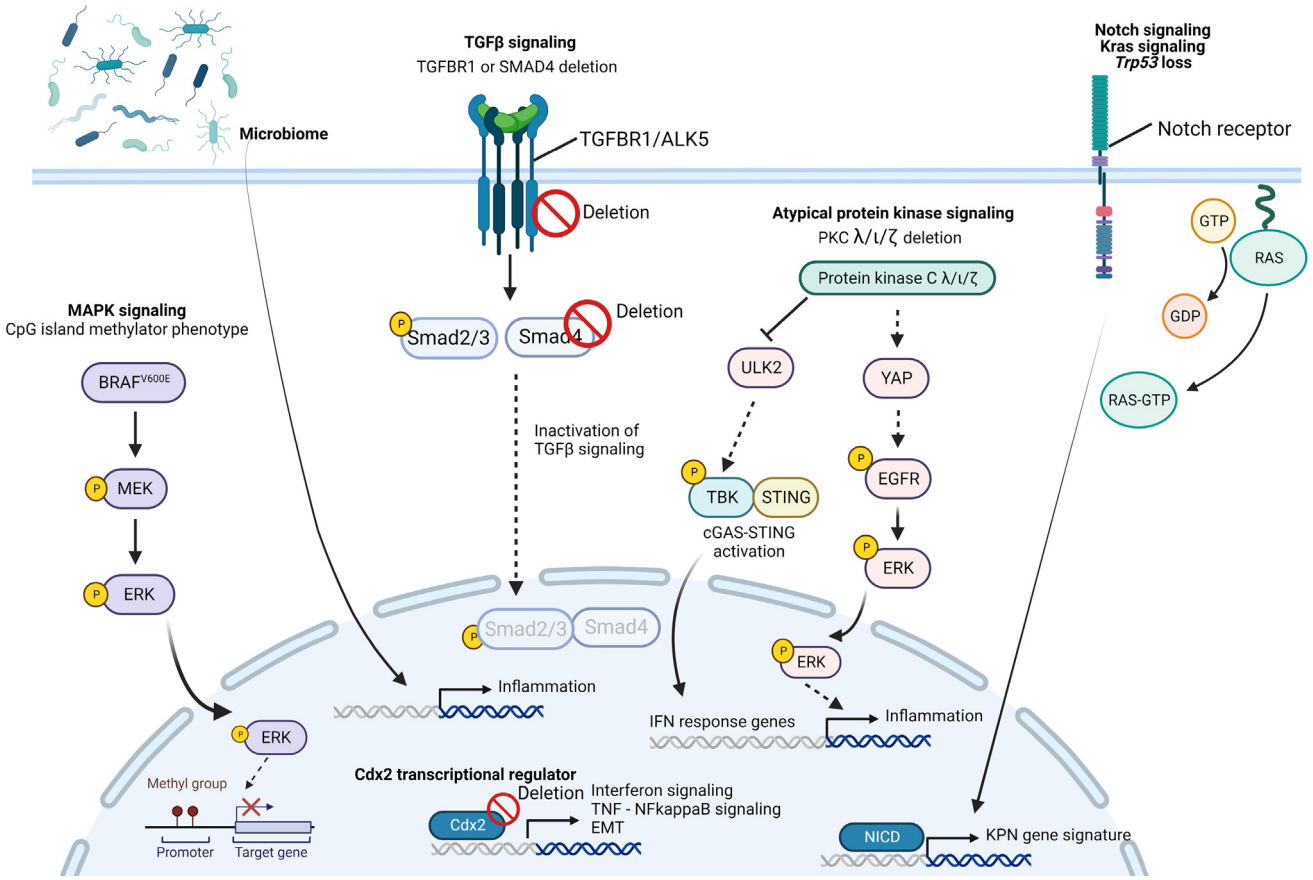

Figure 2. The activation of the MAPK pathway, primarily via BRAF^{V600E}, is a key signaling axis in the initiation of serrated lesions. Progression to invasive serrated CRC involves alterations in other pathways, including transforming growth factor (TGF)-β and atypical protein kinase signaling, as well as inflammatory signals induced by the microbiome. Abbreviations: cGAS-STING, cyclic GMP-AMP synthase and stimulator of interferon genes; EGFR, epidermal growth factor receptor; EMT, epithelial-to-mesenchymal transition; ERK, extracellular signal-regulated kinase; IFN, interferon; KPN, Kras^{G12D}; *Trp53*$^{fl/fl}$; Rosa26$^{N1icd/+}$; MAPK, mitogen-activated protein kinase; P, phosphorylation; TNF, tumor necrosis factor.

section, we highlight the genetic events necessary for progression of Braf^{V600E}-induced lesions into invasive disease (Figure 2, Key figure, and Figure 3).

Trp53 and Cdkn2a loss

Activation of Braf results in senescence, which was bypassed by deletion of *Cdkn2a* [25], suggesting that bypassing the cell cycle checkpoint is one mechanism of disease progression. The *TP53* gene, while having multiple roles in tumorigenesis, functions as a key regulator of the cell cycle [46]. In another study, *Vil-Cre;Braf*$^{LSL-V637E/+}$;*p53*$^{LSL-R172H/+}$ mice had a similar number of dysplasia lesions compared with *Vil-Cre;Braf*$^{LSL-V637E/+}$ counterparts, albeit the former had more invasive carcinomas relative to *Vil-Cre;Braf*$^{LSL-V637E/+}$ mice. Furthermore, *Vil-Cre;Braf*$^{LSL-V637E/+}$; *p16*^{Ink4a*} and *Vil-Cre;Braf*$^{LSL-V637E/+}$ mice did not differ in the number of serrated adenomas, but presented a sixfold

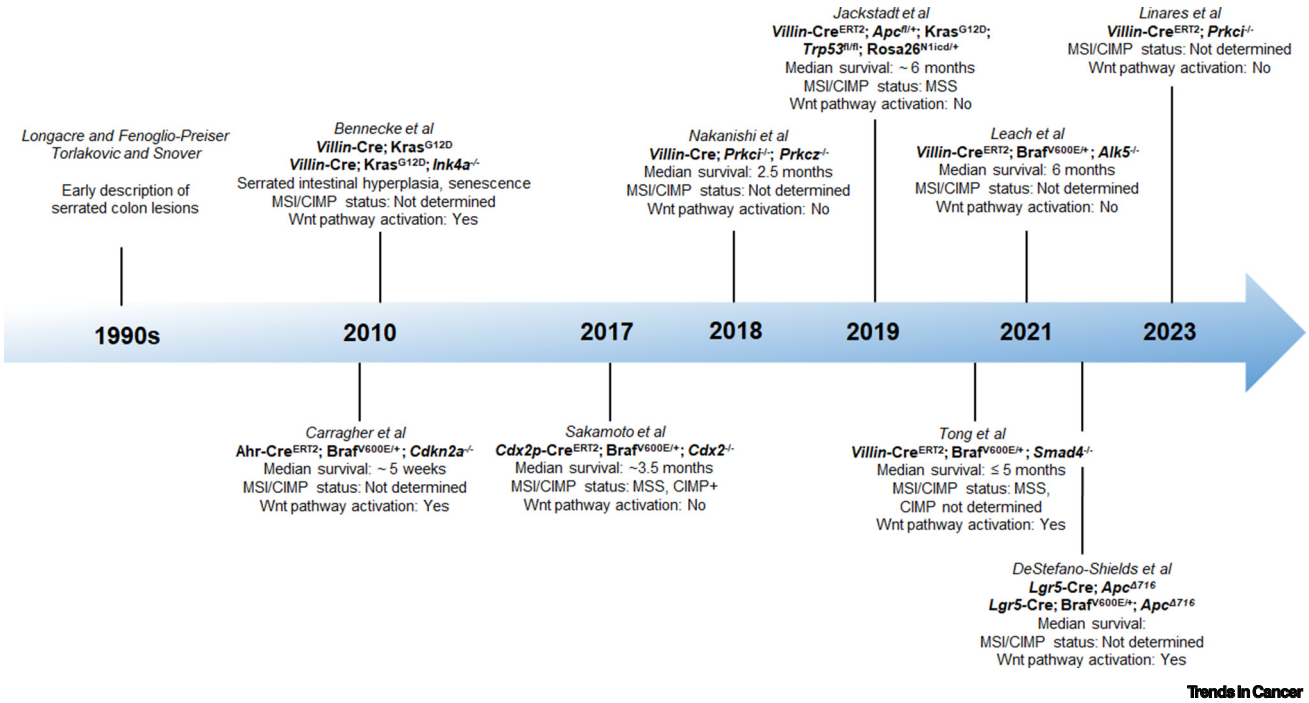

Figure 3. Timeline of studies discussed that investigated the genetic events driving serrated colorectal cancer (CRC) progression. Median survival, microsatellite instability (MSI), CpG island methylator phenotype (CIMP), and Wnt pathway statuses are indicated where available for each study. Longacre and Fenoglio-Preiser [1], Torlakovic and Snover [3], Carragher *et al.* [25], Bennecke *et al.* [29], Sakamoto *et al.* [83], Tong *et al.* [48], Leach *et al.* [49], Nakanishi *et al.* [60], Linares *et al.* [61], Jackstadt *et al.* [65], DeStefano-Shields *et al.* [71].

increase in carcinoma incidence, on average, some of which were metastatic. It is worth noting that *TP53* mutations are infrequent in serrated polyps [47], and the frequency of gain-of-function $p53^{R172H}$ mutations in serrated polyps or carcinomas is poorly characterized. Nevertheless, these findings suggest that inactivation of cell cycle regulators such as p53 and p16 can drive malignant progression of serrated adenomas driven by Braf *in vivo*.

Dedifferentiation associated signaling

Mutations in the transforming growth factor (TGF)-β pathway occur in at least 30% of BRAF mutant CRC and serrated polyps [47,48]. However, the contribution of TGF-β pathway activation to the progression of serrated CRC is largely unexplored. Two recent studies developed genetically engineered mouse models to investigate how loss of different TGF-β pathway members cooperates with Braf activation to drive serrated CRC development. The first reported a conditional knockout of the *Alk5/Tgfbr1* or *Tgfbr2* in mice with intestinal activation of Braf using the Vil-Cre^{ERT2} line [49]. The median tumor-free survival after *Alk5* loss or Braf activation alone was 475–485 days after tamoxifen treatment, suggesting that inactivation of TGF-β or activation of MAPK signaling pathway *per se* forms tumors inefficiently with long latency. However, compound $Braf^{V600E}$ activation and *Alk5* loss ($Braf^{V600E}$; $Alk5^{fl/fl}$) was 192 days, indicating a cooperative effect between the two signaling pathways. While the $Braf^{V600E}$ tumors were primarily in the small intestine, the tumors from $Braf^{V600E}$; $Alk5^{fl/fl}$ arose predominantly in the proximal colon. The $Braf^{V600E}$; $Alk5^{fl/fl}$ tumors had negligible expression of *Notum*, *Lgr5*, or *Axin2*, suggesting that the Wnt signaling pathway is not active in these lesions. Given the low $Lgr5^{+}$ cell population size in the $Braf^{V600E}$; $Alk5^{fl/fl}$ tumors, the authors asked whether the lesions may exhibit a previously identified Lrg5-independent fetal-like differentiation signature (e.g., the *Anxa* and *Ly6* family of genes), which was previously observed during regeneration in response to ionizing radiation or

dextran sulfate sodium (DSS) treatment [50]. Indeed, RNA-sequencing analysis performed on the Braf^{V600E}; *Alk5*$^{fl/fl}$ tumors and the *Villin*^{CreER} proximal colon control tissues revealed a strong enrichment of the fetal-like signature. Furthermore, *in situ* hybridization analysis of the Braf^{V600E}; *Alk5*$^{fl/fl}$ tumors showed selected genes in the fetal signature, such as *Ly6a*, *Anxa1*, and *Krt7*, were expressed exclusively in the tumor epithelium. This fetal signature was turned on 30 days after Alk5 loss and Braf activation, suggesting that it may function early during tumor initiation. Notably, a Braf^{V600E}; *Alk5*$^{fl/fl}$ tumor gene signature generated by the authors was positively correlated with human right-sided CRC tumors that were BRAF mutant and classified as the CMS1 subtype. Thus, Braf activation together with Alk5 loss drives a fetal signature and development of right-sided colon carcinoma. It is worthwhile mentioning that Braf^{V600E} *per se* was sufficient to induce the fetal signature but formed tumors inefficiently. However, it is not clear whether the induction of this fetal signature drives serrated CRCs in the Braf^{V600E}; *Alk5*$^{fl/fl}$ model or is part of an underlying process that includes turning on these genes. Since these fetal signature genes were expressed primarily in the epithelial cells, it may be possible that they adopt a more primitive, dedifferentiated state that might predispose them to transformation.

A second study generated Vil-Cre^{ERT2}; Braf$^{V600E/+}$; Smad4^{KO} mice and assessed the kinetics of serrated CRC development [48]. Consistent with a previous report, macroscopic tumors could be observed as early as 2 months in the Vil-Cre^{ERT2}; Braf$^{V600E/+}$; Smad4^{KO} mice [51]. However, most of these tumors arose in the small intestine, although the proximal colon mucosa was larger, and the epithelial tissue displayed hyperplasia. Microsatellite analysis revealed that these tumors are MSS, unlike the MSI tumors that arose in the Braf^{V600E}; *Alk5*$^{fl/fl}$ tumors described earlier, suggesting that alterations in different components of the TGF-β pathway have different effects on the microsatellite status of tumors. Indeed, analysis of the AACR GENIE dataset revealed that tumors with BRAF^{V600E} and *SMAD4* mutations have approximately one order of magnitude lower mutational burden than BRAF^{V600E} tumors with mutations in other TGF-β pathway members. Importantly, introducing *Msh2* knockout into the Vil-Cre^{ERT2}; Braf$^{V600E/+}$; Smad4^{KO} mice increased tumor and mutational burden, suggesting that additional mutations accelerated tumor development. Exome sequencing analysis revealed frequent activating mutations in *Ctnnb1* and elevated Wnt signaling in both the Vil-Cre^{ERT2}; Braf$^{V600E/+}$; Smad4^{KO} and the Vil-Cre^{ERT2}; Braf$^{V600E/+}$; Smad4^{KO}; Msh2^{KO} models. This finding contrasts with the Braf^{V600E}; *Alk5*$^{fl/fl}$ model, which did not exhibit activation of the Wnt signaling pathway. Additionally, it is not clear whether the fetal signature identified in the Braf^{V600E}; *Alk5*$^{fl/fl}$ mice was present in this Braf$^{V600E/+}$; Smad4^{KO} model. Thus, alterations in different members of the TGF-β signaling may differentially require Wnt signaling to accelerate serrated CRC development, likely via different mechanisms.

CDX2 encodes a homeodomain transcription factor from the caudal-related family of genes and has roles in alimentary tract specification during embryonic development and intestinal cell proliferation, differentiation, adhesion, and apoptosis [52]. The Cdx2 protein is expressed from the proximal duodenum to distal rectum and has been reported as a potential biomarker for CRCs with features that closely associate with the serrated pathway [53,54]. However, a causative role for *Cdx2* loss in serrated CRC development was unappreciated. To this end, a study assessed for an association between *KRAS* and *BRAF* mutations and CDX2 expression in CRC tissues and determined a significant co-occurrence between CDX2 reduction and activating *BRAF* mutation. On the basis of this association, the authors used the *Cdx2p*-Cre line to activate Braf^{V600E} and/or delete *Cdx2*. The median survival of mice with either Braf activation or *Cdx2* deletion was 480 days, whereas compound activation of Braf and *Cdx2* deletion resulted in median survival of 103 days. Mice with either Braf activation or *Cdx2* deletion exhibited marked intestinal hyperplasia, whereas Braf^{V600E} activation and *Cdx2* deletion resulted in large tumors (>10 mm) and multiple polypoid lesions at the ileocecal and proximal colon junction. The Braf^{V600E};

Cdx2$^{-/-}$ tumors had both serrated and mucinous histological features, and the serrated component had cytological features that closely associated with human serrated CRC. Isolation of DNA from either the mucinous or serrated regions revealed that the serrated regions had both Braf^{V600E} activation and *Cdx2* deletion, whereas the mucinous regions only had *Cdx2* deletion. In Braf^{V600E}; *Cdx2*$^{-/-}$ mice, between 17% and 50% of the lesions showed invasion of the serrated glands into the submucosa, indicative of carcinomas. To glean mechanistic insights, RNA-sequencing analysis of colon epithelium from Braf^{V600E} only, *Cdx2*$^{-/-}$ only, and Braf^{V600E}; *Cdx2*$^{-/-}$ revealed several pathways as being selectively enriched in the latter, including interleukin (IL)/STAT- and tumor necrosis factor (TNF)/NF-κB–associated pathways, suggesting that enhanced inflammation features strongly influence tumorigenesis.

Inflammation-associated signaling

Inflammation is a key component of CRC development [55]. One potential mechanism of how inflammation may regulate tumorigenesis is via a feedforward loop that involves the telomerase enzyme [56,57]. The atypical protein kinase C λ/I, encoded by *PRKCI*, has been shown to regulate inflammation in the context of chronic inflammatory bowel diseases, such as Crohn's disease and ulcerative colitis, which may progress to invasive CRC [58,59]. Knockout of *Prkci* in the presence of inflammation was insufficient to drive colorectal tumorigenesis, unless combined with *Apc* deficiency. One possible explanation is that a second atypical protein kinase, PKCζ, encoded by *PRKCZ*, may compensate for the loss of *Prkci* and induce tumor-suppressive pathways that mitigate tumor initiation and progression. To test this, intestine-specific compound knockout of *Prkci* and *Prkcz* (*Vil-Cre*;Prkci$^{fl/fl}$; Prkcz$^{fl/fl}$) was generated, and the small intestine and colon tissues exhibited a 'sawtoothed' appearance that resembles the human serrated phenotype, with cytomorphologic features resembling human goblet cell-rich or microvesicular serrated hyperplasia [60]. Furthermore, in the *Vil-Cre*;Prkci$^{fl/fl}$; Prkcz$^{fl/fl}$ mice, both the small intestine and colon developed SSA/P, which was not observed in either *Vil-Cre*;Prkci$^{fl/fl}$ or *Vil-Cre*;Prkcz$^{fl/fl}$ alone, and these lesions progressed to tumors over time. Thirteen (81%) of 16 mice developed tumors in the colon, which were enriched in the proximal side, consistent with the behavior of human serrated CRC. These tumors were MSS, with no observable changes in expression of genes involved in DNA repair (i.e., mismatch repair proficient), and CIMP-negative. The SSA/P and adenocarcinoma lesions from *Vil-Cre*;Prkci$^{fl/fl}$;Prkcz$^{fl/fl}$ did not display nuclear accumulation of β-catenin, and enrichment analysis performed on transcriptome data from *Vil-Cre*;Prkci$^{fl/fl}$;Prkcz$^{fl/fl}$ tumors revealed positive enrichment for MEK, EGFR, and RAS gene signatures.

The *Vil-Cre*;Prkci$^{fl/fl}$; Prkcz$^{fl/fl}$ tumors displayed extensive infiltration of CD45$^+$ cells, suggesting a strong immune response associated with tumorigenesis. The CD45$^+$ cells exhibited strong expression of programmed death-ligand 1 (PD-L1), a significant increase in Foxp3$^+$ regulatory T cells and accumulation of CD11b$^+$ myeloid cells, including both Ly6C^{hi}Ly6G$^-$ monocytic cells and Ly6C$^+$Ly6G$^+$ polymorphonuclear cells, which suggest the presence of myeloid-derived suppressor cells. Additionally, compound *Prkci* and *Prkcz* loss resulted in decreased infiltration of CD8$^+$ T cells, and these cytotoxic T cells were excluded from the SSA/P and adenocarcinoma areas of the tumors. The limited CD8$^+$ T cell presence can be explained by decreased expression of genes involved in interferon signaling in the *Vil-Cre*;Prkci$^{fl/fl}$; Prkcz$^{fl/fl}$, which is primarily due to loss of *Prkcz* compared with wild-type control. These observations suggest that dual *Prkci* and *Prkcz* loss results in an immunosuppressive tumor microenvironment. Consistent with its tumor suppressive role, intestinal deletion of *Prkci*, together with dextran sodium sulfate/azoxymethane treatment, resulted in smaller tumors with elevated interferon signaling and recruitment of CD8 T cells, compared with mice with basal *Prkci* expression [61]. A series of biochemical experiments revealed that Pkcλ/I interacts with ULK2, a kinase that phosphorylates TBK1, to activate the

cyclic GMP-AMP synthase (cGAS) and stimulator of interferon genes (STING) pathway and interferon signaling. The Pkcλ/I-ULK2 interaction serves to reduce the latter activity by inducing ubiquitin-lysosome degradation, thereby reducing ULK2 stability and abundance. Thus, *Prkci* loss has the dual role of promoting tumorigenesis and immunosurveillance, which may be considered for immunomodulatory treatment strategies.

Notch signaling and metastasis

Serrated CRC can be classified into the CMS4 molecular subtype, which is characterized by a mesenchymal profile [e.g., TGF-β signaling activation, cancer-associated fibroblast (CAF) abundance, epithelial-to-mesenchymal transition (EMT), angiogenesis, innate immune cell activation] and enrichment in *KRAS* mutations [62]. The Notch signaling pathway has been implicated in inflammation and CRC and can be activated by ligands from tumor cells, endothelial cells, or innate immune cells [63,64]. High NOTCH score was associated with CMS4 subtype and poor prognosis, and a high proportion of CRC metastasis exhibited strong staining for the Notch intracellular domain [65]. Several mouse models with alleles that included *Vil*-CreERT2; $Apc^{fl/+}$; $Kras^{G12D}$; $Trp53^{fl/fl}$; $Rosa26^{N1icd/+}$ were developed to investigate how KRAS mutations cooperate with Notch signaling to drive CRC *in vivo*. Tumor incidence was similar between $Apc^{fl/+}$; $Trp53^{fl/fl}$ (AP), $Apc^{fl/+}$; $Trp53^{fl/fl}$; $Rosa26^{N1icd/+}$ (APN), $Kras^{G12D}$; $Trp53^{fl/fl}$ (KP) and $Kras^{G12D}$; $Trp53^{fl/fl}$; $Rosa26^{N1icd/+}$ (KPN). By contrast, $Trp53^{fl/fl}$; $Rosa26^{N1icd/+}$ (PN) mice developed tumors with extended latency. Histologically, the KPN tumors exhibited serrated morphology, whereas tumors with *Apc* loss displayed tubular morphology, and the KPN tumors retained *MLH1* expression, suggesting that these tumors represent serrated intestinal tumors with an MSS phenotype.

The gene expression signature derived from KPN and APN tumors and organoids revealed that the KPN signature predicted poorer outcome. Moreover, a neutrophil infiltration signature was observed in KPN tumors. Chemokine analysis to identify mediators of neutrophil attractant revealed *Cxcl5* expressed in tumor epithelial cells and increased *Cxcr2* expression in neutrophils. Pharmacological blockade of the CXCR2 receptor or neutrophil depletion in KPN mice markedly reduced metastasis, without affecting primary tumor burden. Curiously, no significant difference in survival was observed in response to these treatments, raising the question of to what degree neutrophil-associated metastasis contributes to the demise of KPN mice. Additionally, *Tgfb2* expression was upregulated in KPN organoids and *TGFB2* expression was associated with CMS4, NOTCH score, KPN/KP signature, and serrated type in human CRC datasets. Inhibition of the TGF-β signaling pathway using an ALK5 inhibitor reduced metastasis burden and neutrophil infiltration in these lesions. Furthermore, ALK5 or CXCR2 inhibition increased cytotoxic CD8 T cell abundance in metastatic lesions, suggesting that reduced neutrophil abundance and increased antitumor CD4 and CD8 cells may drive antimetastatic effects.

The gut microbiome in serrated CRC development

CRC risk factors have been associated with changes in the composition and function of the local ecosystem comprising bacteria, fungi, archaea, and virus, collectively known as the microbiome. Serrated lesions often exhibit increased expression of various mucins, which produces a mucus cap that may sustain the microbiota [66]. Furthermore, identifying enrichment and/or depletion of specific strains may facilitate studies to decipher how the microbiota cooperate with genetic hits to drive serrated CRC.

Bacterial biofilm was detected in 89% of right-sided normal and CRC tissues, compared with 12% in left-sided tumors [67]. The presence of these invasive microbial biofilms was associated with increased epithelium permeability, elevated IL6–STAT3 activation, and enhanced crypt epithelial cell proliferation. Additional studies have performed deeper analysis of the microbiome

between conventional (enriched in left side) and serrated (enriched in right side) CRC. Sequencing of 16S rDNA between conventional adenoma and serrated lesions from 540 individuals (323 controls, 144 conventional, 40 HP, 33 SSL) that underwent colonoscopy observed a significant reduction in *Erysipelotrichia* in SSL, compared with control. However, independent studies performed on an Iranian and a South Korean cohort did not detect any notable differences in the microbiome composition between normal control, HP, and SSL, which may be attributed to smaller sample sizes [68,69].

To annotate the microbiome more comprehensively between conventional and serrated polyps, 1883 samples were collected from 140 individuals (50 polyp-free, 45 tubular adenoma, 33 serrated adenoma, 12 unknown pathology) using a combination of sampling methods, including mucosal brushes and aspirates, lavage aspirates, and fecal samples. Sampling methods (e.g., from the colon mucosa vs. feces) were found to account for 10–15% of microbiome variation. At the individual level, mucosal brushings between healthy intestinal tissues and polyps did not reveal significant differences in microbiome composition. However, mucosal aspirates from tubular adenomas and serrated polyps were significantly different between each other, as well as polyp-free individuals, accounting for 1–4% of variation in the microbiome. Importantly, a classifier model developed from the microbiome profile demonstrated accurate prediction of polyp types (i.e., tubular vs. serrated), suggesting robust microbiome differences between the different polyp types.

Despite these broad correlations of microbiome and different CRC tumor types, functional evidence for the role of the microbiome in serrated CRC development is sparse. One study noted *Prkci*-knockout intestinal epithelium resulted in an inflammatory state and altered microbiome profile, with increased abundance of *Proteobacteria* and decreased *Firmicutes* [60]. Furthermore, intestinal tumors from $Apc^{fl/+}$; $Prkcl^{KO}$ mice exhibited a marked increase in inflammatory cytokines, compared with $Apc^{fl/+}$ tumors, and $Apc^{fl/+}$; $Prkcl^{KO}$ treated with a broad-spectrum antibiotic cocktail resulted in a significant reduction in tumor multiplicity, compared with only $Apc^{fl/+}$. Thus, these findings suggest an interplay between inflammation and microflora in the development of $Apc^{fl/+}$; $Prkcl^{KO}$-driven intestinal and colon tumors. Separately, $Braf^{V600E}$; $Alk5^{fl/fl}$ mice displayed compromised integrity of the mucosal barrier, which may expose the epithelium to gut microbiota and toxic metabolites to trigger inflammation. Indeed, treatment with broad-spectrum antibiotics also significantly reduced tumor burden and extended survival only for mice with right-sided tumors. RNA-sequencing analysis of antibiotic- and vehicle-treated $Braf^{V600E}$; $Alk5^{fl/fl}$ tissues revealed reduction in pathways involved in inflammation and immune response. Interestingly, expression of the fetal-like gene program was also reduced in response to antibiotic treatment compared with vehicle control. Collectively, these findings suggest that inflammation and the gut microflora are key features in driving $Braf^{V600E}$; $Alk5^{fl/fl}$ or *Prkci* and *Prkcz* knockout-driven serrated tumorigenesis.

Several strains of bacteria have been implicated in colorectal carcinogenesis, such as *Escherichia coli* that expresses polyketide synthase, enterotoxigenic *Bacteroides fragilis* (ETBF), and *Fusobacterium nucleatum* [70]. ETBF colonization resulted in colitis in $Braf^{V600E}$; $Lgr5^{Cre}$ (BL) mice, whereas long-term ETBF colonization resulted in increased splenic and liver inflammation, albeit with no tumor formation [71]. Up to 16 weeks of age, tumorigenesis in $Apc^{\Delta 716}$-Min or $Braf^{V600E}$; $Lgr5^{Cre}$; $Apc^{\Delta 716}$ (BLM) was generally rare and restricted to the distal colon. ETBF colonization for 6–13 weeks resulted in tumor formation in the distal colon for Min mice, whereas BLM mice presented tumors in the midproximal and distal colon, and longer-term ETBF colonization resulted in double the median tumor burden in BLM, compared with Min mice. Notably, the midproximal tumors were unique to $Braf^{V600E}$ as $Kras^{G12D}$; $Lgr5^{Cre}$, Min mice gave rise to only distal colon tumors, like Min only mice. Global CpG island methylation analysis

revealed marked increases in DNA methylation in either $Apc^{\Delta 716}$-Min or BLM mice with ETBF colonization, compared with either genotype with sham exposure. However, ETBF-induced BLM tumors exhibited increased CpG island methylation compared with $Apc^{\Delta 716}$-Min tumors + ETBF and their respective sham controls. RNA-sequencing analysis performed on Apc^{Min} and BLM sham epithelium revealed that BLM epithelium was enriched for genes involved in interferon signaling, and ETBF-induced BLM tumors were enriched for gene sets associated with T-helper 1 and IL12/Stat4 signaling, compared with ETBF + $Apc^{\Delta 716}$-Min tumors. Altogether, these findings demonstrate that pathogenic bacteria colonization cooperates with the genetic background to modulate the epigenetic and gene expression status, as well as the location, of colorectal tumors. Consistent with enhanced immune cell migration and signaling in the ETBF-induced BLM tumors, anti-PD-L1 treatment significantly reduced tumor burden compared with isotype-treated control. By contrast, there was no significant difference in the number of tumors between ETBF + $Apc^{\Delta 716}$-Min mice treated with anti-PD-L1 or isotype control. Collectively, these findings support further investigation of how pathogenic microbiota cooperates with host intestinal genetics to drive serrated CRC and potential response to immune checkpoint blockade.

Concluding remarks and future perspectives

We anticipate that the first wave of studies discussed earlier will help guide the development of subsequent *in vitro* and *in vivo* models that will provide mechanistic insights into disease biology. However, several challenges and limitations remain (see Outstanding questions). Specifically, the cellular origins and gene–environment interactions associated with the initiation and progression of serrated CRC remains poorly understood. We highlight future areas to study and gain fundamental insights into disease biology and identify new therapeutic avenues (Figure 4).

Metaplasia is the replacement of a resident differentiated cell with another differentiated cell type not present in the tissue [72]. A common example is intestinal metaplasia, which can occur in several tissues, including esophagus, gastric, or pancreas, in response to injury. Metaplasia occurs as part of the repair process, but, if unresolved, it can potentiate tumorigenesis [72,73]. Multiomic analyses of conventional and serrated polyps identified a gastric metaplasia gene signature (e.g., *MUC5AC*, *AQP5*, *TFF2*, and *MSLN*) enriched in the latter. Furthermore, serrated adenomas exhibited a reduced stemness score, which led to the authors proposing that these lesions arise from a 'top-down' manner as opposed to the 'bottom-up' stem cell driven model associated with conventional colorectal adenoma/carcinoma development. The $Lgr5^{+}$ population in the intestinal crypt has been demonstrated to be the cell of origin in intestinal cancers [74]. Presumably, the 'top-down' model would suggest a non-stem/progenitor (i.e., *LGR5*-negative) cell of origin for initiation of serrated adenoma. What is the cell of origin, and what are the subsequent (epi)genetic alterations selected in this non-stem population? This question requires a thoughtful approach as the cell of origin is likely to arise from a confluence of several factors, including underlying mutations, and external cues such as inflammation, and the local microenvironment, such as the stromal cells and the microbiome. Furthermore, tumor site (e.g., proximal vs. distal) and the junctional zones, such as the ileocecal junction, may have different propensities for transformation and distinct cell of origin [75].

The commonly used *Vil*-Cre model targets most cells that line the crypt–villus axis, which may limit understanding the cell of origin for serrated CRC. The *Mist1*-Cre line that target cell types outside of the colonic crypt base (e.g., goblet/enteroendocrine cells) was shown to predispose tumor development in the proximal colon [47]. Generating other Cre lines that target specific cell types along the crypt–base axis together with cell-lineage tracing studies may illuminate the cellular origins of serrated CRC. Therefore, it will be important to explore whether the gastric metaplasia observed in human serrated adenoma is essential for disease development or a

Outstanding questions

What is the (epi)genetic evolutionary landscape of serrated colorectal cancer?

What is the tumor microenvironment associated with the different serrated lesions (i.e., sessile serrated, goblet cell rich, microvesicular hyperpolyps)? How does this change during disease progression?

What biomarker/s could serve as a molecular surrogate to identify serrated lesions?

Can we identify genetic promoter/s to develop transgenic Cre line/s that would more effectively target genetic recombination in the proximal colon, where serrated CRC primarily develops?

Why do some genetically engineered mouse models exhibit CIMP, MSI, and Wnt signaling activation and others do not?

What therapeutic vulnerabilities can be targeted in MSI/CIMP serrated tumors? Are these lesions sensitive to DNA-damaging agents, immunotherapy, and/or epigenetic modulators?

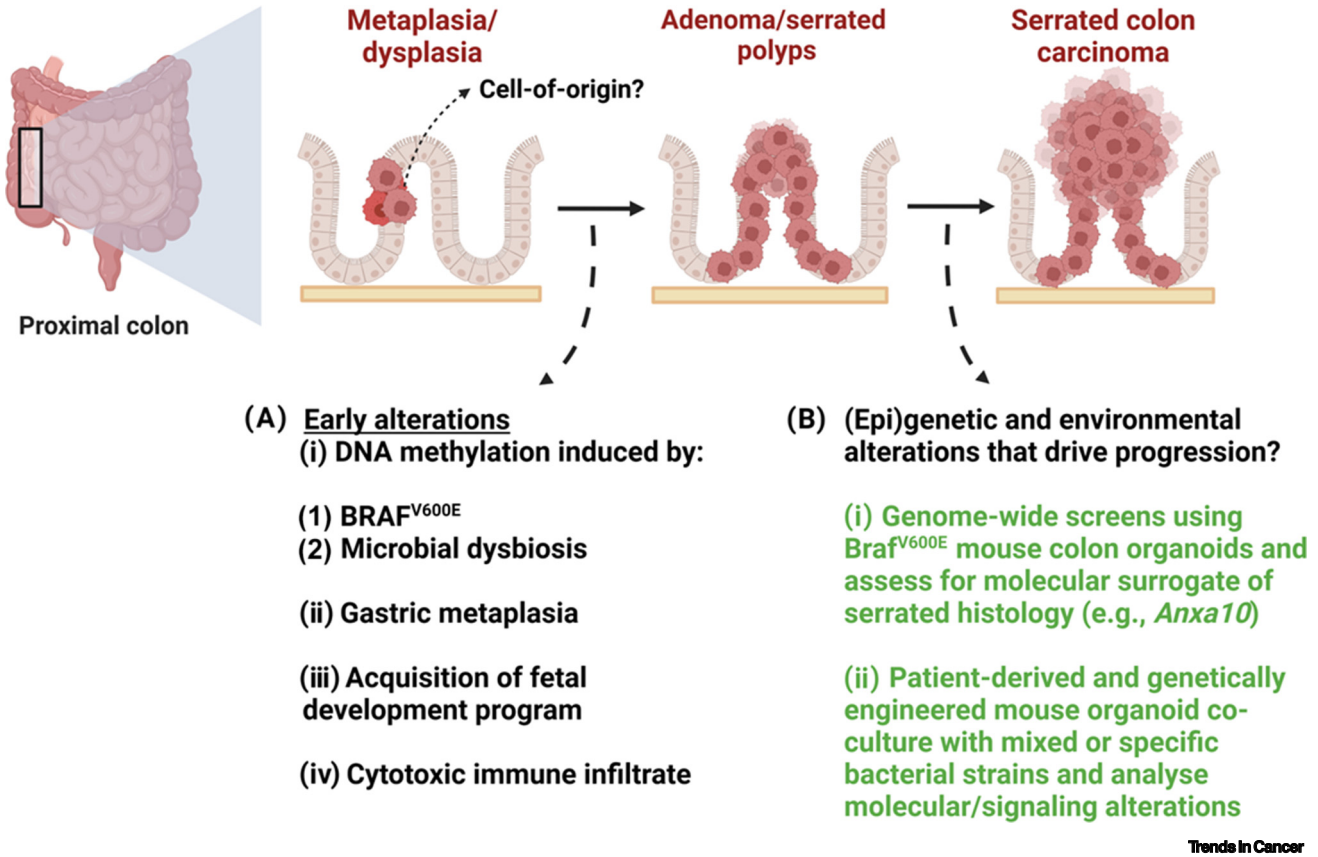

Figure 4. Initiation and progression model of serrated colorectal cancer (CRC). (A) The early events associated with serrated polyps/adenoma from mouse models and patient material analysis. (B) The progression events remain poorly defined and may benefit from unbiased genetic screens and using organoid models that may provide a time- and cost-effective platform to assess features to investigate further using *in vivo* models.

consequence of early tissue damage. The identification of key transcriptional node/s driving the gastric metaplasia and generating knockouts of such factors in genetically engineered mouse organoids (e.g., Braf^{V600E} + Cdx2$^{-/-}$) will be crucial in addressing this problem. These organoids can then be transplanted orthotopically and monitored for tumorigenesis as well as be used for in-depth molecular analyses. Alternatively, reporter primary cell lines and organoids can be generated for genome-wide screens to identify regulators of gastric metaplasia in these systems [76,77].

While conventional and serrated polyps have been profiled [78], it is unclear whether the strains identified are associated with progression to invasive serrated CRC. Thus, a systematic, longitudinal clinical study that tracks the evolution of the gut microbiome in healthy individuals and individuals with serrated lesions that do or do not progress to invasive cancers may have potential translational relevance for early detection and microbiome supplementation. Once specific strains associated with disease progression are identified, they can be cocultured with patient- or mouse-derived serrated tumor organoids for histology, DNA-sequencing, and RNA-sequencing analyses to delineate the molecular programs of host tumor–microbiome interaction. Alternatively, genetically engineered mice with oncogenic alleles can be housed in a germ-free environment and dosed with strains depleted or enriched in serrated CRC and monitored for tumor development. In-depth analysis such as single-cell and spatial transcriptome analysis can be performed to assess for tumor–environment interactions [79].

Treatment strategies and protocols for patients with serrated CRC are less defined relative to conventional CRC. Some areas that have been proposed for therapeutic targeting include angiogenic signaling, immune checkpoint inhibitors, and blocking the FASCN protein at the invasive front [80]. However, randomized clinical studies that assess these agents are required to determine the efficacy and patient outcome during and after treatment. Serrated CRC may present with specific features, such as mesenchyme involvement (e.g., desmoplasia), that could be therapeutically amenable. The *Vil-Cre*;*Prkci*$^{fl/fl}$; *Prkcz*$^{fl/fl}$ model results in serrated tumors with desmoplasia and a molecular profile similar to CMS4 and iCMS3 mesenchymal CRC [81]. Treatment with pegylated hyaluronidase (PEGPH) resulted in reduced tumor burden *in vivo*, and single-cell analyses revealed marked changes in the fibroblast composition between treated and untreated tumors. Furthermore, PEGPH treatment sensitized tumors to immune checkpoint blockade and reduced liver metastatic lesions. Separately, MMR deficiency is a common feature of serrated CRC. In this regard, a small neoadjuvant study conducted on patients with rectal carcinoma with dMMR tumors demonstrated excellent efficacy to anti-PD-L1 treatment, which could be explored in the treatment of serrated CRC in the clinical setting [82]. Altogether, these examples highlight the importance of modelling the heterogeneous features of serrated CRC, with the goal to better understand disease biology and identify potential therapeutic avenues.

Acknowledgments

A.A. and V.T. are supported by the Agency for Science, Technology and Research (A*STAR), BMRC Central Research Fund - User Inspired Basic Research (UIBR) award, National Research Foundation (NRF) award no. NRF-CRP26-2021-0001, and National Medical Research Council (NMRC) award no. OFIRG21jun-0101. N.B. is supported A*STAR, BMRC Central Research Fund -UIBR award and NMRC award no. OFIRG19may-0069. We thank Dorcas Hei for assistance with figure design in this article.

Declaration of interests

The authors declare no competing interests.

References

1. Longacre, T.A. and Fenoglio-Preiser, C.M. (1990) Mixed hyperplastic adenomatous polyps/serrated adenomas. A distinct form of colorectal neoplasia. *Am. J. Surg. Pathol.* 14, 524–537
2. Goldstein, N.S. *et al.* (2003) Hyperplastic-like colon polyps that preceded microsatellite-unstable adenocarcinomas. *Am. J. Clin. Pathol.* 119, 778–796
3. Torlakovic, E. *et al.* (2003) Morphologic reappraisal of serrated colorectal polyps. *Am. J. Surg. Pathol.* 27, 65–81
4. Iino, H. *et al.* (1999) DNA microsatellite instability in hyperplastic polyps, serrated adenomas, and mixed polyps: a mild mutator pathway for colorectal cancer? *J. Clin. Pathol.* 52, 5–9
5. Kambara, T. *et al.* (2004) BRAF mutation is associated with DNA methylation in serrated polyps and cancers of the colorectum. *Gut* 53, 1137–1144
6. O'Brien, M.J. *et al.* (2006) Comparison of microsatellite instability, CpG island methylation phenotype, BRAF and KRAS status in serrated polyps and traditional adenomas indicates separate pathways to distinct colorectal carcinoma end points. *Am. J. Surg. Pathol.* 30, 1491–1501
7. Szylberg, L. *et al.* (2015) Serrated polyps and their alternative pathway to the colorectal cancer: a systematic review. *Gastroenterol. Res. Pract.* 2015, 573814
8. Nishihara, R. *et al.* (2013) Long-term colorectal-cancer incidence and mortality after lower endoscopy. *N. Engl. J. Med.* 369, 1095–1105
9. Burgess, N.G. *et al.* (2014) Sessile serrated adenomas/polyps with cytologic dysplasia: a triple threat for interval cancer. *Gastrointest. Endosc.* 80, 307–310
10. Arain, M.A. *et al.* (2010) CIMP status of interval colon cancers: another piece to the puzzle. *Am. J. Gastroenterol.* 105, 1189–1195
11. Lee, Y.M. and Huh, K.C. (2017) Clinical and biological features of interval colorectal cancer. *Clin. Endosc.* 50, 254–260
12. Nagtegaal, I.D. *et al.* (2020) The 2019 WHO classification of tumours of the digestive system. *Histopathology* 76, 182–188
13. Yan, H.H.N. *et al.* (2017) RNF43 germline and somatic mutation in serrated neoplasia pathway and its association with BRAF mutation. *Gut* 66, 1645–1656
14. Yamamoto, D. *et al.* (2022) Characterization of RNF43 frameshift mutations that drive Wnt ligand- and R-spondin-dependent colon cancer. *J. Pathol.* 257, 39–52
15. Vilar, E. and Gruber, S.B. (2010) Microsatellite instability in colorectal cancer-the stable evidence. *Nat. Rev. Clin. Oncol.* 7, 153–162
16. De Sousa, E.M.F. *et al.* (2013) Poor-prognosis colon cancer is defined by a molecularly distinct subtype and develops from serrated precursor lesions. *Nat. Med.* 19, 614–618
17. Ogino, S. *et al.* (2006) CpG island methylator phenotype (CIMP) of colorectal cancer is best characterised by quantitative DNA methylation analysis and prospective cohort studies. *Gut* 55, 1000–1006
18. Chan, A.O. *et al.* (2002) Concordant CpG island methylation in hyperplastic polyposis. *Am. J. Pathol.* 160, 529–536
19. Weisenberger, D.J. *et al.* (2006) CpG island methylator phenotype underlies sporadic microsatellite instability and is tightly associated with BRAF mutation in colorectal cancer. *Nat. Genet.* 38, 787–793
20. Buikhuisen, J.Y. *et al.* (2020) Exploring and modelling colon cancer inter-tumour heterogeneity: opportunities and challenges. *Oncogenesis* 9, 66
21. Joanito, I. *et al.* (2022) Single-cell and bulk transcriptome sequencing identifies two epithelial tumor cell states and refines the consensus molecular classification of colorectal cancer. *Nat. Genet.* 54, 963–975

22. Honkala, A. *et al.* (2022) Harnessing the predictive power of preclinical models for oncology drug development. *Nat. Rev. Drug Discov.* 21, 99–114
23. Rosenberg, D.W. *et al.* (2007) Mutations in BRAF and KRAS differentially distinguish serrated versus non-serrated hyperplastic aberrant crypt foci in humans. *Cancer Res.* 67, 3551–3554
24. Cantwell-Dorris, E.R. *et al.* (2011) BRAFV600E: implications for carcinogenesis and molecular therapy. *Mol. Cancer Ther.* 10, 385–394
25. Carragher, L.A. *et al.* (2010) V600EBraf induces gastrointestinal crypt senescence and promotes tumour progression through enhanced CpG methylation of p16INK4a. *EMBO Mol. Med.* 2, 458–471
26. Rad, R. *et al.* (2013) A genetic progression model of Braf(V600E)-induced intestinal tumorigenesis reveals targets for therapeutic intervention. *Cancer Cell* 24, 15–29
27. Riemer, P. *et al.* (2015) Transgenic expression of oncogenic BRAF induces loss of stem cells in the mouse intestine, which is antagonized by beta-catenin activity. *Oncogene* 34, 3164–3175
28. Stefanius, K. *et al.* (2011) Frequent mutations of KRAS in addition to BRAF in colorectal serrated adenocarcinoma. *Histopathology* 58, 679–692
29. Bennecke, M. *et al.* (2010) Ink4a/Arf and oncogene-induced senescence prevent tumor progression during alternative colorectal tumorigenesis. *Cancer Cell* 18, 135–146
30. Rustgi, A.K. (2013) BRAF: a driver of the serrated pathway in colon cancer. *Cancer Cell* 24, 1–2
31. Drost, J. and Clevers, H. (2018) Organoids in cancer research. *Nat. Rev. Cancer* 18, 407–418
32. Fujii, M. *et al.* (2016) A colorectal tumor organoid library demonstrates progressive loss of niche factor requirements during tumorigenesis. *Cell Stem Cell* 18, 827–838
33. Lannagan, T.R.M. *et al.* (2019) Genetic editing of colonic organoids provides a molecularly distinct and orthotopic preclinical model of serrated carcinogenesis. *Gut* 68, 684–692
34. Kawasaki, K. *et al.* (2020) Chromosome engineering of human colon-derived organoids to develop a model of traditional serrated adenoma. *Gastroenterology* 158, 638–651 e8
35. Neal, J.T. *et al.* (2018) Organoid modeling of the tumor immune microenvironment. *Cell* 175, 1972–1988 e16
36. Seino, T. *et al.* (2018) Human pancreatic tumor organoids reveal loss of stem cell niche factor dependence during disease progression. *Cell Stem Cell* 22, 454–467 e6
37. Ohlund, D. *et al.* (2017) Distinct populations of inflammatory fibroblasts and myofibroblasts in pancreatic cancer. *J. Exp. Med.* 214, 579–596
38. Kasashima, H. *et al.* (2021) Stromal SOX2 upregulation promotes tumorigenesis through the generation of a SFRP1/2-expressing cancer-associated fibroblast population. *Dev. Cell* 56, 95–110 e10
39. Martinez-Ordonez, A. *et al.* (2023) Whole-mount staining of mouse colorectal cancer organoids and fibroblast-organoid co-cultures. *STAR Protoc.* 4, 102243
40. Bettington, M. *et al.* (2017) Clinicopathological and molecular features of sessile serrated adenomas with dysplasia or carcinoma. *Gut* 66, 97–106
41. Tanaka, H. *et al.* (2006) BRAF mutation, CpG island methylator phenotype and microsatellite instability occur more frequently and concordantly in mucinous than non-mucinous colorectal cancer. *Int. J. Cancer* 118, 2765–2771
42. Fang, M. *et al.* (2014) The BRAF oncoprotein functions through the transcriptional repressor MAFG to mediate the CpG island methylator phenotype. *Mol. Cell* 55, 904–915
43. Bond, C.E. *et al.* (2018) Oncogenic BRAF mutation induces DNA methylation changes in a murine model for human serrated colorectal neoplasia. *Epigenetics* 13, 40–48
44. Tao, Y. *et al.* (2019) Aging-like spontaneous epigenetic silencing facilitates Wnt activation, stemness, and Braf(V600E)-induced tumorigenesis. *Cancer Cell* 35, 315–328 e6
45. Fennell, L. *et al.* (2022) *Braf* mutation induces rapid neoplastic transformation in the aged and aberrantly methylated intestinal epithelium. *Gut* 71, 1127–1140
46. Engeland, K. (2022) Cell cycle regulation: p53-p21-RB signaling. *Cell Death Differ.* 29, 946–960
47. Chen, B. *et al.* (2021) Differential pre-malignant programs and microenvironment chart distinct paths to malignancy in human colorectal polyps. *Cell* 184, 6262–6280 e26
48. Tong, K. *et al.* (2021) SMAD4 is critical in suppression of BRAF-V600E serrated tumorigenesis. *Oncogene* 40, 6034–6048
49. Leach, J.D.G. *et al.* (2021) Oncogenic BRAF, unrestrained by TGFbeta-receptor signalling, drives right-sided colonic tumorigenesis. *Nat. Commun.* 12, 3464
50. Yui, S. *et al.* (2018) YAP/TAZ-dependent reprogramming of colonic epithelium links ECM remodeling to tissue regeneration. *Cell Stem Cell* 22, 35–49 e7
51. Tong, K. *et al.* (2017) Degree of tissue differentiation dictates susceptibility to BRAF-driven colorectal cancer. *Cell Rep.* 21, 3833–3845
52. Saad, R.S. *et al.* (2011) CDX2 as a marker for intestinal differentiation: its utility and limitations. *World J. Gastrointest. Surg.* 3, 159–166
53. Lee, J.A. *et al.* (2022) Comprehensive clinicopathologic, molecular, and immunologic characterization of colorectal carcinomas with loss of three intestinal markers, CDX2, SATB2, and KRT20. *Virchows Arch.* 480, 543–555
54. Landau, M.S. *et al.* (2014) BRAF-mutated microsatellite stable colorectal carcinoma: an aggressive adenocarcinoma with reduced CDX2 and increased cytokeratin 7 immunohistochemical expression. *Hum. Pathol.* 45, 1704–1712
55. Schmitt, M. and Greten, F.R. (2021) The inflammatory pathogenesis of colorectal cancer. *Nat. Rev. Immunol.* 21, 653–667
56. Ozturk, M.B. *et al.* (2017) Current insights to regulation and role of telomerase in human diseases. *Antioxidants (Basel)* 6, 17
57. Ghosh, A. *et al.* (2012) Telomerase directly regulates NF-kappaB-dependent transcription. *Nat. Cell Biol.* 14, 1270–1281
58. Nakanishi, Y. *et al.* (2016) Control of Paneth cell fate, intestinal inflammation, and tumorigenesis by PKClambda/iota. *Cell Rep.* 16, 3297–3310
59. Akincilar, S.C. *et al.* (2021) NAIL: an evolutionarily conserved lncRNA essential for licensing coordinated activation of p38 and NFkappaB in colitis. *Gut* 70, 1857–1871
60. Nakanishi, Y. *et al.* (2018) Simultaneous loss of both atypical protein kinase C genes in the intestinal epithelium drives serrated intestinal cancer by impairing immunosurveillance. *Immunity* 49, 1132–1147 e7
61. Linares, J.F. *et al.* (2021) PKClambda/iota inhibition activates an ULK2-mediated interferon response to repress tumorigenesis. *Mol. Cell* 81, 4509–4526 e10
62. Guinney, J. *et al.* (2015) The consensus molecular subtypes of colorectal cancer. *Nat. Med.* 21, 1350–1356
63. Tyagi, A. *et al.* (2020) A review on Notch signaling and colorectal cancer. *Cells* 9, 1549
64. Ang, H.L. and Tergaonkar, V. (2007) Notch and NFkappaB signaling pathways: do they collaborate in normal vertebrate brain development and function? *BioEssays* 29, 1039–1047
65. Jackstadt, R. *et al.* (2019) Epithelial NOTCH signaling rewires the tumor microenvironment of colorectal cancer to drive poor-prognosis subtypes and metastasis. *Cancer Cell* 36, 319–336 e7
66. Walsh, M.D. *et al.* (2013) Expression of MUC2, MUC5AC, MUC5B, and MUC6 mucins in colorectal cancers and their association with the CpG island methylator phenotype. *Mod. Pathol.* 26, 1642–1656
67. Dejea, C.M. *et al.* (2014) Microbiota organization is a distinct feature of proximal colorectal cancers. *Proc. Natl. Acad. Sci. U. S. A.* 111, 18321–18326
68. Yoon, H. *et al.* (2017) Comparisons of gut microbiota among healthy control, patients with conventional adenoma, sessile serrated adenoma, and colorectal cancer. *J. Cancer Prev.* 22, 108–114
69. Rezasoltani, S. *et al.* (2018) The association between fecal microbiota and different types of colorectal polyp as precursors of colorectal cancer. *Microb. Pathog.* 124, 244–249
70. Clay, S.L. *et al.* (2022) Colorectal cancer: the facts in the case of the microbiota. *J. Clin. Invest.* 132, e155101
71. DeStefano Shields, C.E. *et al.* (2021) Bacterial-driven inflammation and mutant BRAF expression combine to promote murine

colon tumorigenesis that is sensitive to immune checkpoint therapy. *Cancer Discov.* 11, 1792–1807
72. Giroux, V. and Rustgi, A.K. (2017) Metaplasia: tissue injury adaptation and a precursor to the dysplasia-cancer sequence. *Nat. Rev. Cancer* 17, 594–604
73. Saenz, J.B. (2021) Follow the metaplasia: characteristics and oncogenic implications of metaplasia's pattern of spread throughout the stomach. *Front. Cell Dev. Biol.* 9, 741574
74. Barker, N. *et al.* (2009) Crypt stem cells as the cells-of-origin of intestinal cancer. *Nature* 457, 608–611
75. Mukund, K. *et al.* (2020) Right and left-sided colon cancers - specificity of molecular mechanisms in tumorigenesis and progression. *BMC Cancer* 20, 317
76. Katti, A. *et al.* (2022) CRISPR in cancer biology and therapy. *Nat. Rev. Cancer* 22, 259–279
77. Shanmugam, R. *et al.* (2022) Genome-wide screens identify specific drivers of mutant *hTERT* promoters. *Proc. Natl. Acad. Sci. U. S. A.* 119, e2105171119
78. Avelar-Barragan, J. *et al.* (2022) Distinct colon mucosa microbiomes associated with tubular adenomas and serrated polyps. *NPJ Biofilms Microbiomes* 8, 69
79. Galeano Nino, J.L. *et al.* (2022) Effect of the intratumoral microbiota on spatial and cellular heterogeneity in cancer. *Nature* 611, 810–817
80. Alburquerque-Gonzalez, B. *et al.* (2020) Biology and therapeutic targets of colorectal serrated adenocarcinoma; clues for a histologically based treatment against an aggressive tumor. *Int. J. Mol. Sci.* 21, 1991
81. Martinez-Ordonez, A. *et al.* (2023) Hyaluronan driven by epithelial aPKC deficiency remodels the microenvironment and creates a vulnerability in mesenchymal colorectal cancer. *Cancer Cell* 41, 252–271 e9
82. Cercek, A. *et al.* (2022) PD-1 blockade in mismatch repair-deficient, locally advanced rectal cancer. *N. Engl. J. Med.* 386, 2363–2376
83. Sakamoto, N. *et al.* (2017) $BRAF^{V600E}$ cooperates with CDX2 inactivation to promote serrated colorectal tumorigenesis. *eLife* 6, e20331